Sequence current controllability analysis of an offshore MMC-HVDC during asymmetrical faults

Heng Wu and Xiongfei Wang
Dept. of Energy Technology
Aalborg University
Aalborg, Denmark
hew, xwa@et.aau.dk

Jesper Hjerrild, Łukasz H.Kocewiak and Lorenzo Zeni
Wind Power
Ørsted
Fredericia, Denmark
jeshj, lukko, lorze@ orsted.dk

***Abstract*—This paper analyzes the sequence current controllability of an offshore MMC-HVDC during asymmetrical faults. It is found that the separate limitation of the output positive- and negative-sequence current of the MMC-HVDC during asymmetrical faults may encounter physical limitations of the external faulted network, which leads to the sequence currents being out of control and the possible overcurrent tripping of the MMC-HVDC. To tackle this challenge, a fault ride through control method of the MMC-HVDC that limits its phase current and phase modulation signal is proposed in this paper, with which the magnitude of the fault current can be effectively limited. Time-domain simulations are given to confirm the effectiveness of the proposed method.**

Keywords—Asymmetrical fault, offshore MMC-HVDC, sequence current control

I. INTRODUCTION

Offshore modular multilevel converter (MMC) based high-voltage direct current (HVDC) transmission systems are increasingly adopted for integrating offshore wind farms (OWFs) into the power system. In order to guarantee the reliable operation of the whole system, fault ride through (FRT) capability of both the OWF and the offshore MMC-HVDC is required. Fault current injection requirement of the OWF has been clearly specified in the grid codes [1]-[3]. At the beginning, only the positive-sequence reactive current injection of the OWF was required during symmetrical and asymmetrical faults [1]-[2], while the additional requirement for the negative-sequence reactive current injection during asymmetrical faults has been added in more recent grid codes [3]. A number of control solutions of the OWF to fulfill this requirement are also available in the literature [4].

In contrast, currently there are few grid codes specifying sequence current injection requirement for offshore MMC-HVDC during asymmetrical faults. In [5] and [6], it is pointed out that injecting pure positive-sequence current during asymmetrical faults is not applicable for the offshore MMC-HVDC, otherwise unrealistically high phase voltages can be observed. However, the control dynamics of the offshore MMC-HVDC is not considered in [5] and [6]. With the modulation signal limitation block which is always adopted in the HVDC control, the phase overvoltage will not occur, but on the other hand the sequence currents will not be controlled to the desired values.

In order to facilitate future standardization of the sequence current injection of offshore MMC-HVDC during asymmetrical faults, this paper performs a systematic study on its sequence current controllability. Different from [5] and [6], the control dynamics of the offshore MMC-HVDC is considered during the analysis. It is found that the separate limitation of the output positive- and negative-sequence current of the MMC-HVDC during asymmetrical faults is not feasible, due to the constraints of the external faulted network, which is in accordance with the findings in [5]-[6]. However, the arbitrary settling of the positive- and negative-sequence current control commands will saturate the modulation signal limitation block in the MMC-HVDC, which on the one hand avoids the phase overvoltage described in [5]-[6], but on the other hand further drifts the actual output sequence currents away from their command values. As a result, the actual output sequence currents are out of control, and may lead to the overcurrent tripping of the offshore MMC-HVDC.

In order to avoid the overcurrent tripping described above, this paper further introduces a FRT method for offshore MMC-HVDC by limiting the current and modulation signals on per-phase basis, rather than limiting their positive- and negative-sequence components. By doing so, the offshore MMC-HVDC can successfully ride through the asymmetrical fault with the phase current magnitude under control, while the percentage of the positive- and negative-sequence currents are determined by the external faulted network. Time domain simulation are given to verify the effectiveness of the proposed method.

II. SYSTEM DESCRIPTION

Fig. 1 illustrates the system configuration of the OWF connected to the offshore MMC-HVDC through step-up transformers. The faults on the 155kV submarine cables are considered in this study. For simplicity, the OWF is aggregated as one wind turbine (WT) converter.

Fig. 2 shows the standard control scheme of the offshore MMC-HVDC [7], in which the cascaded outer voltage loop and inner current loop are adopted to control both the positive- and negative-sequence components of the MMC. v_{MMC}, i_{MMC} and m_{ac} are output voltage, output current and modulation signals of the MMC, respectively. Hereafter in this paper, the subscript p and n represent the positive- and negative-sequence component, respectively. As shown in Fig. 2, the positive/negative sequence current references and modulation signals are separately limited to avoid the over current and over modulation of the MMC. During the fault,

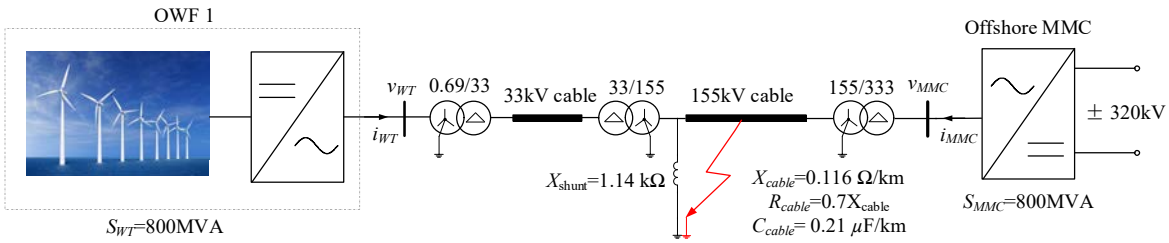

Fig. 1. System configuration of the OWF connected to the offshore MMC-HVDC

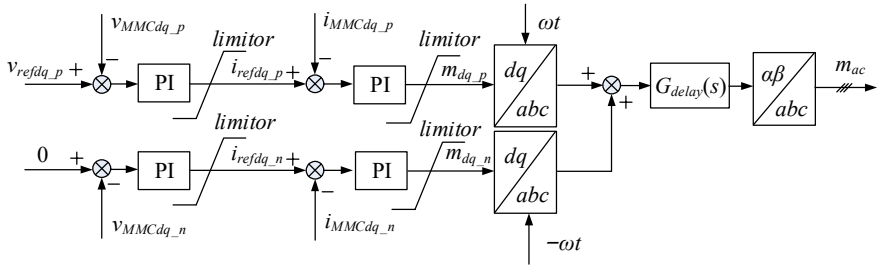

Fig. 2. Standard control scheme of the voltage controlled MMC

the voltage regulators are saturated due to the persistent errors between the voltage references and the actual output voltages of the MMC, which leads to the current references of the inner current loops being equal to the limiting values, and the MMC is supposed to naturally switch to the current control mode to limit its output current.

III. Fault Analysis

A. Sequence Network During Asymmetrical Faults

Fig. 3 illustrates the sequence network of the system during a single-line to ground fault [8]. The current controlled WT converter is modeled as a controlled current source, while the voltage controlled MMC is modeled as a controlled voltage source. Z_{MMC} and Z_{WT} are the equivalent impedances of the MMC and the wind farm seen from the fault location, respectively. v_f and i_f are the voltage and current at the fault location, respectively.

Based on Fig. 3, the relationship of sequence voltages and currents can be derived as follows:

$$i_{fp} = i_{fn} = i_{f0} . \quad (1.1)$$

$$i_{MMCp} = i_{fp} - i_{WTp} . \quad (1.2)$$

$$v_{fp} = v_{MMCp} - i_{MMCp} Z_{MMCp} . \quad (1.3)$$

$$i_{MMCn} = i_{fn} - i_{WTn} = i_{fp} - i_{WTn} . \quad (1.4)$$

$$v_{fn} = v_{MMCn} - i_{MMCn} Z_{MMCn} . \quad (1.5)$$

$$i_{MMC0} = i_{f0} - i_{WT0} = i_{fp} - i_{WT0} . \quad (1.6)$$

$$v_{f0} = -i_{WT0} Z_{WT0} = -i_{MMC0} Z_{MMC0} . \quad (1.7)$$

$$v_{fp} + v_{fn} + v_{f0} = 0 . \quad (1.8)$$

Based on (1.1)-(1.8), the fault current can be calculated as:

$$i_{fp} = i_{fn} = i_{f0} = \frac{v_{MMCp} + v_{MMCn} + i_{WTp} Z_{MMCp} + i_{WTn} Z_{MMCn}}{Z_{MMCp} + Z_{MMCn} + \frac{Z_{MMC0} Z_{WT0}}{Z_{MMC0} + Z_{WT0}}} . \quad (2)$$

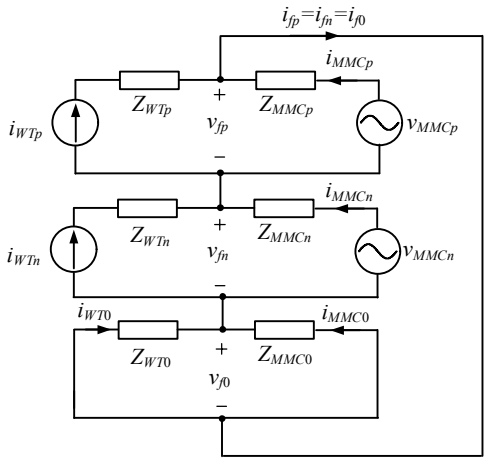

Fig. 3. Sequence network of the system during the single-line to ground fault

Fig. 4 shows the sequence network of the system during a line-to-line fault [8], and the relationship of sequence voltages and current can be expressed as:

$$i_{fp} = -i_{fn} . \quad (3.1)$$

$$i_{MMCp} = i_{fp} - i_{WTp} . \quad (3.2)$$

$$v_{fp} = v_{MMCp} - i_{MMCp} Z_{MMCp} . \quad (3.3)$$

$$i_{MMCn} = i_{fn} - i_{WTn} = -i_{fp} - i_{WTn} . \quad (3.4)$$

$$v_{fn} = v_{MMCn} - i_{MMCn} Z_{MMCn} . \quad (3.5)$$

$$v_{fp} = v_{fn} . \quad (3.6)$$

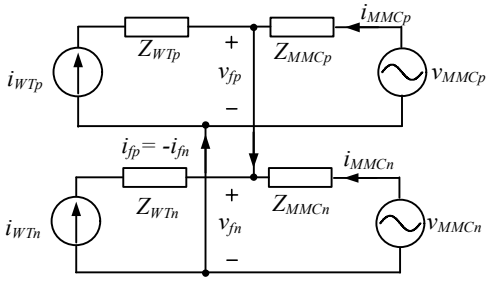

Fig. 4. Sequence network of the system during the line-to-line fault

and the fault current can be calculated as:

$$i_{fp} = -i_{fn} = \frac{v_{MMCp} - v_{MMCn} + i_{WTp}Z_{MMCp} - i_{WTn}Z_{MMCn}}{Z_{MMCp} + Z_{MMCn}} . \quad (4)$$

Fig. 5 shows the sequence network of the system during the double-line to ground fault [8], and the relationship of sequence voltages and current can be expressed as:

$$i_{fp} = -i_{fn} - i_{f0} . \quad (5.1)$$

$$i_{MMCp} = i_{fp} - i_{WTp} . \quad (5.2)$$

$$v_{fp} = v_{MMCp} - i_{MMCp}Z_{MMCp} . \quad (5.3)$$

$$i_{MMCn} = i_{fn} - i_{WTn} . \quad (5.4)$$

$$v_{fn} = v_{MMCn} - i_{MMCn}Z_{MMCn} . \quad (5.5)$$

$$i_{MMC0} = i_{f0} - i_{WT0} = -i_{fp} - i_{fn} - i_{WT0} \quad (5.6)$$

$$v_{f0} = -i_{WT0}Z_{WT0} = -i_{MMC0}Z_{MMC0} \quad (5.7)$$

$$v_{fp} = v_{fn} = v_{f0} . \quad (5.8)$$

and the fault current can be calculated as:

$$i_{fp} = \frac{v_{MMCp}Z_{eq} - v_{MMCn} + i_{WTp}Z_{MMCp}Z_{eq} - i_{WTn}Z_{MMCn}}{Z_{MMCp}Z_{eq} + Z_{MMCn}} . \quad (6)$$

$$i_{fn} = \frac{v_{MMCp} + i_{WTp}Z_{MMCp}}{Z_{p0}} - i_{fp}\left(1 + \frac{Z_{MMCp}}{Z_{p0}}\right). \quad (7)$$

$$i_{f0} = -i_{fp} - i_{fn}$$

where:

$$Z_{p0} = \frac{Z_{MMC0}Z_{WT0}}{Z_{MMC0} + Z_{WT0}} . \quad (8)$$

$$Z_{eq} = 1 + \frac{Z_{MMCn}}{Z_{p0}} . \quad (9)$$

B. Control Interactions

As discussed in Section III-A, the sequence network during the asymmetrical faults bring additional constraints on the sequence components. However, these constraints may be compromised if the standard control scheme of the MMC shown in Fig. 2 is adopted, in which the positive- and negative-sequence components are controlled independently. As will be illustrated in the following, the conflict between the MMC control dynamics and the physical limitation of the sequence network will lead to uncontrollability of the sequence currents of the MMC, which induces the risk of the overcurrent tripping.

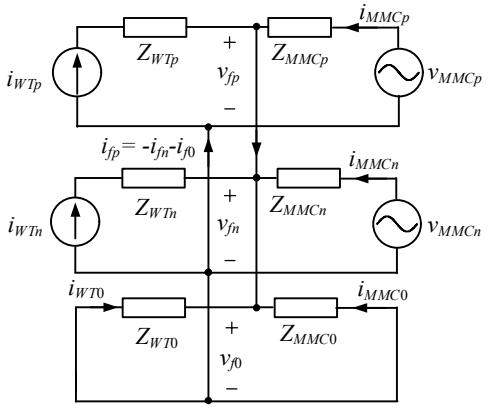

Fig. 5. Sequence network of the system during the double-line to ground fault.

A single-line to ground fault is considered here as an example. For simplicity, the WT converter is assumed not connected, which corresponds to the operating scenario that the MMC energizes the transformers and submarine cables. During the single-line to ground fault, the output voltage of the MMC is asymmetrical, i.e., $V_{MMCdq\_p} \neq V_{refdq\_p}$, $V_{MMCdq\_n} \neq 0$. As shown in Fig. 2, these persistent voltage errors lead to the output of the positive- and negative-sequence voltage regulator saturated to i_{refdq_plim} and i_{refdq_nlim}, and the MMC control naturally switches to the current limiting mode with the positive- and negative-sequence current references as i_{refdq_plim} and i_{refdq_nlim} .

On the other hand, the output sequence currents of the MMC should meet the constraints determined by the sequence network. As $i_{WTp}=i_{WTn}=0$, the relationship of the sequence components shown in (1.1)-(1.8) and (2) can be simplified as:

$$i_{fp} = i_{fn} = i_{f0} = \frac{v_{MMCp} + v_{MMCn}}{Z_{MMCp} + Z_{MMCn} + Z_{p0}} . \quad (10)$$

$$i_{MMCp} = i_{fp} . \quad (11)$$

$$i_{MMCn} = i_{fp} . \quad (12)$$

It is observed in (10)-(12) that $i_{MMCp}=i_{MMCn}=i_{fp}$ is required. However, i_{refdq_plim} and i_{refdq_nlim} are set solely for limiting the current of the MMC; and there is no requirement of $i_{refdq\_plim} = i_{refdq\_nlim.}$ Therefore, the conflict between the control dynamics of the MMC and physical constraints of the network occurs in case of $i_{refdq\_plim} \neq i_{refdq\_nlim}$, which leads to three possible operation scenarios.

i) $i_{MMCp}=i_{MMCn}= i_{ref\_plim} \neq i_{ref\_nlim}$. In this case, the negative-sequence modulation signal will be saturated to m_{nlim} due to the persistent current error in the negative-sequence current control, which leads to $v_{MMCn} = v_{MMCnlim.}$ Based on (10), v_{MMCp} can be calculated as:

$$v_{MMCp} = i_{refp\_\lim}\left(Z_{MMCp} + Z_{MMCn} + Z_{p0}\right) - v_{MMCn\lim} . \quad (13)$$

This operating scenario will take place if v_{MMCp} calculated based on (13) is within its voltage limit.

ii) Similarly, if $i_{MMCp}=i_{MMCn}= i_{ref\_nlim} \neq i_{ref\_plim}$, the positive sequence modulation signal will be saturated to m_{plim}, and v_{MMCn} can be calculated as:

$$v_{MMCn} = i_{refn\_\lim}\left(Z_{MMCp} + Z_{MMCn} + Z_{p0}\right) - v_{MMCp\lim} . \quad (14)$$

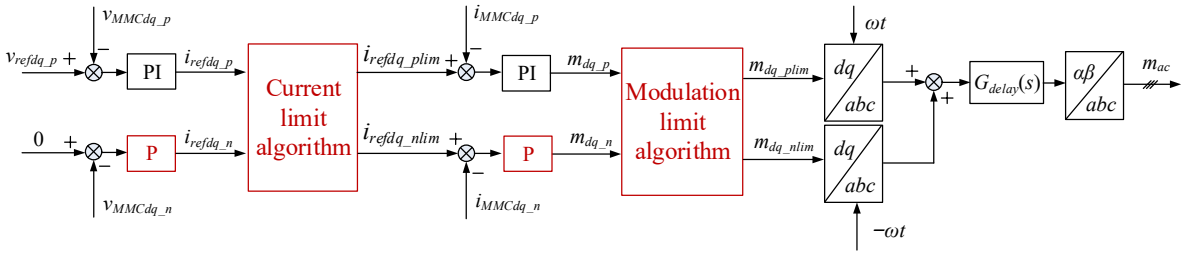

Fig. 6. Proposed control scheme of the voltage controlled MMC

This operating scenario will take place if v_{MMCn} calculated based on (14) is within its voltage limit.

iii) If neither i) nor ii) are satisfied, i_{MMCp} and i_{MMCn} will neither equal to i_{ref_plim} nor i_{ref_nlim}. In this case, both the positive- and negative-sequence modulation signals will be saturated to m_{plim} and m_{nlim}, and thus the output sequence current of the MMC can be calculated as:

$$i_{MMCp} = i_{MMCn} = i_{fp} = \frac{v_{MMCp\,\lim} + v_{MMCn\,\lim}}{Z_{MMCp} + Z_{MMCn} + Z_{p0}}. \quad (15)$$

It is known from i)-iii) that at least one sequence current will be out of control by using the separate sequence limitation schemes shown in Fig. 2. Therefore, the actual output current of the MMC cannot be limited by simply limiting its sequence current references i_{refdq_p} and i_{refdq_n} .

The same problem will also be encountered during a line-to-line fault and a double-line to ground fault. The basic mechanism of the uncontrollability of the sequence currents is similar and will not be repeated here.

IV. Current Limiting Strategies

As discussed in Section III, the root cause of the poor current controllability of the offshore MMC-HVDC during the asymmetrical fault is the improper setting of i_{ref_plim} and i_{ref_nlim}, which contradicts the sequence current constraints of the network. Theoretically, this problem can be avoided by aligning i_{ref_plim} and i_{ref_nlim} with the real sequence current constraints of the external circuit. However, implementing this method requires the prior knowledge of the fault types, line impedance and the current injection of the WT converter, which is difficult in practice. Therefore, the alternative current limiting strategy is proposed in this paper.

Fig. 6 shows the proposed control scheme of the voltage controlled MMC. There are two basic modifications compared with the standard control scheme shown in Fig.2, which are:

i) The proportional (P) controllers, rather than the proportional integrator (PI) controllers are adopted as the negative-sequence voltage and current controller. It is known from (1.1), (3.1) and (5.1) that there is only one degree of freedom for the sequence current control, i.e., as long as the positive (negative) sequence current is under control, the uncontrolled negative (positive) sequence current will be naturally determined by the external network. Therefore, it is not feasible to simultaneously control the positive- and negative-sequence components without steady-state error by using PI controllers. Hence, the P controllers are used for the negative-sequence components control, which allow the steady-state tracking error of the negative-sequence voltage and current.

ii) The current and modulation limit algorithms are modified. Instead of limiting the positive- and negative-sequence components of the current and modulation signals separately, the proposed method limit the magnitude of the current and modulation signals in per-phase basis, as shown in Fig. 7. The advantage of the proposed method is that it does not manually specify the percentage of the positive- and negative-sequence components during the fault, which alleviates the conflict with the external networks and reduce the risk of uncontrolled quantities. It should be noted that the integrators in the positive-sequence control loop should be clamped when the limit algorithm is activated in order to avoid the windup.

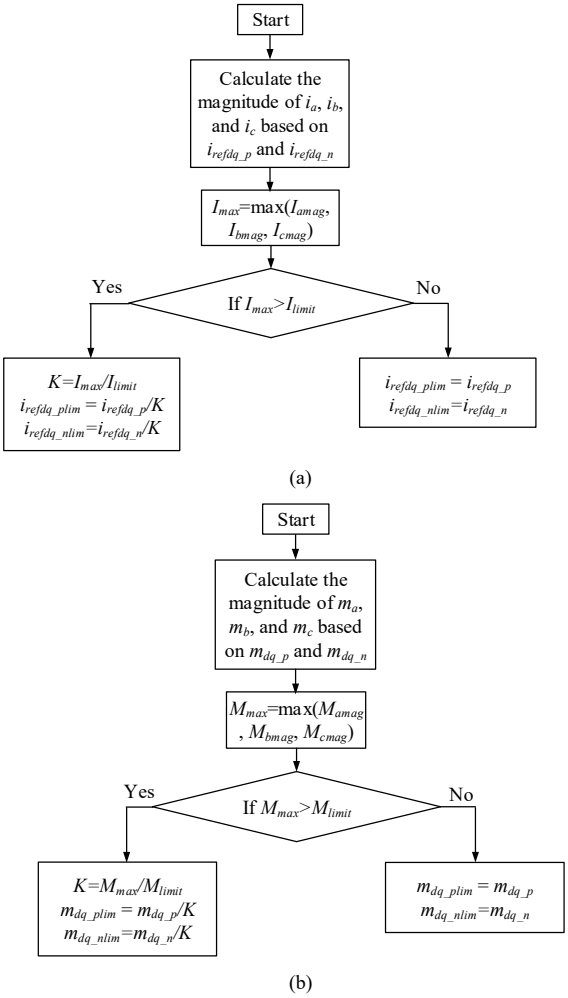

Fig. 7. (a) Current limitation algorithm. (b) Modulation signal limitation algorithm.

The magnitude of three phase currents can be calculated based on its dq components [4], which are given as follows:

$$I_{amag} = \sqrt{I_p^2 + I_n^2 + 2I_pI_n\cos\left(\theta_p + \theta_n\right)}$$
$$I_{bmag} = \sqrt{I_p^2 + I_n^2 + 2I_pI_n\cos\left(\theta_p + \theta_n - \frac{4}{3}\pi\right)}. \quad (16)$$
$$I_{cmag} = \sqrt{I_p^2 + I_n^2 + 2I_pI_n\cos\left(\theta_p + \theta_n + \frac{4}{3}\pi\right)}$$

where

$$I_p = \sqrt{i_{dp}^2 + i_{qp}^2}, \quad I_n = \sqrt{i_{dn}^2 + i_{qn}^2}. \quad (17)$$

$$\theta_p = \arctan\frac{i_{qp}}{i_{dp}}, \quad \theta_n = \arctan\frac{i_{qn}}{i_{dn}}. \quad (18)$$

The magnitude of modulation signals can also be calculated similarly and will not be repeated here.

V. Simulation Results

In order to verify the effectiveness of the proposed method, time-domain simulations are carried out based on the electromagnetic transient (EMT) model shown in Fig. 1. Since the focus of this paper is the sequence current controllability of the offshore MMC-HVDC. For simplicity, the pure positive-sequence current injection of the WT converter during the fault is assumed in this study, where its active and reactive current references are specified by the grid code [1]. The dynamic response of the offshore MMC-HVDC with the standard control scheme shown in Fig. 2 and the proposed control scheme shown in Fig. 6 are investigated and compared.

Fig. 8 shows the simulation results of the system during the single-line to ground fault. The standard control scheme of the MMC shown in Fig. 2 is adopted, which limits the positive- and negative-sequence components separately. In the simulation, i_{ref_plim}=1.5 pu, i_{ref_nlim}=0.15 pu, m_{plim}=1.2 pu and m_{nlim}=0.15 pu are adopted. The fault occurs at t=0.6s and is cleared at t=0.8s.

Fig. 8(a) shows the sequence voltages and currents at the fault location, it is clear that positive-, negative-, and zero-sequence currents are almost identical, which confirms the constraints shown in (1.1). The WT converter also injects 1 pu positive-sequence current as expected, as shown in Fig. 8(b). However, although the positive- and negative-sequence current references of the MMC are limited to 1.5 pu and 0.15 pu, its actual output positive- and negative-sequence currents are out of control due to the constraints of the external network, as shown in Fig. 8(c). The corresponding time-domain waveforms in Fig. 8(d) illustrate that the maximum phase current of the MMC reaches approximately 3.8 pu during the fault, which will lead to the overcurrent tripping in the real application. The simulation results shown in Fig. 8 clearly show that the standard control scheme of the MMC with the separate sequence current limitation cannot limit the actual output current of the MMC during the asymmetrical faults.

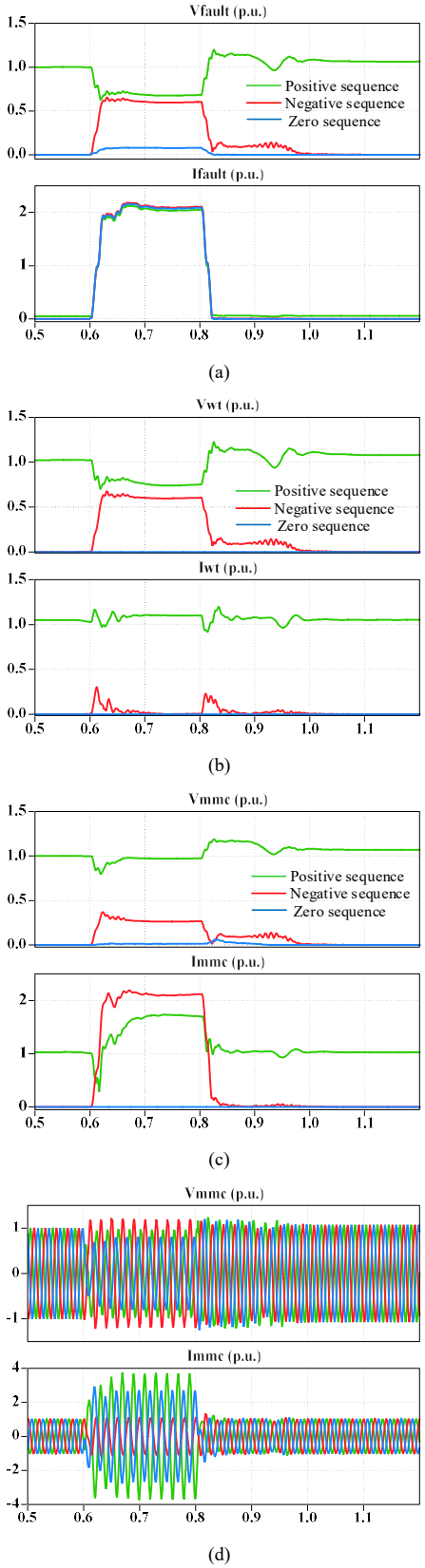

Fig. 8. Simulation results of the system during a single-line to ground fault, the standard control scheme of the MMC shown in Fig.2 is used. (a) Sequence voltage and current at the fault location. (b) Sequence voltage and current of the WT converter. (c) Sequence voltage and current of the MMC. (d) Time-domain waveform of the MMC.

Fig. 9 shows the simulation results of the system during the single-line to ground fault. The proposed control scheme of the MMC shown in Fig. 6 is adopted, which limits the current and modulation signals in per-phase basis. The current limitation is set as 1.5 pu while the modulation signal limitation is set as 1.2 pu. Time domain waveforms in Fig. 9 (d) shows that the maximum magnitude of the phase currents is 1.2 pu during the fault, which is within the limiting value (1.5 pu). The time-domain simulation results confirm the effectiveness of the proposed method.

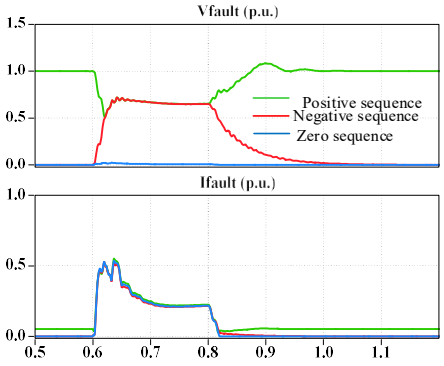

(a)

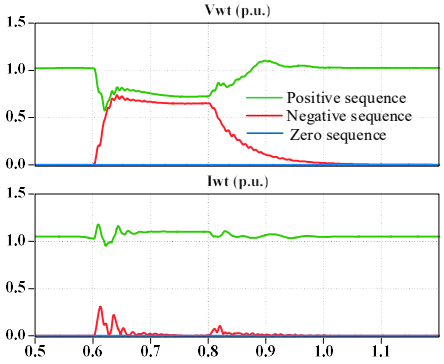

(b)

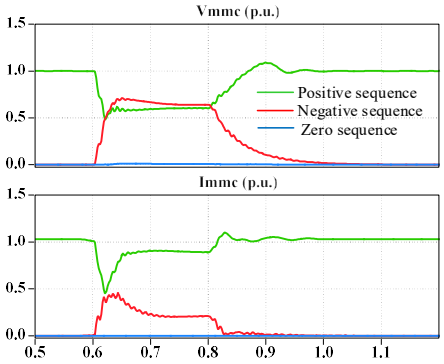

(c)

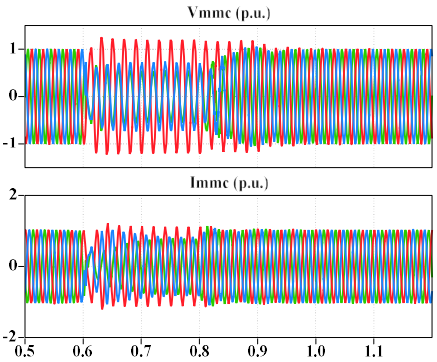

(d)

Fig. 9. Simulation results of the system during a single-line to ground fault, the proposed control scheme of the MMC shown in Fig.6 is used. (a) Sequence voltage and current at the fault location. (b) Sequence voltage and current of the WT converter. (c) Sequence voltage and current of the MMC. (d) Time-domain waveform of the MMC.

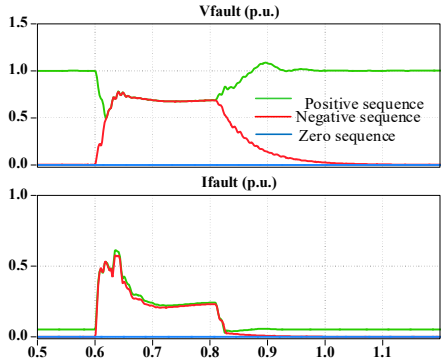

(a)

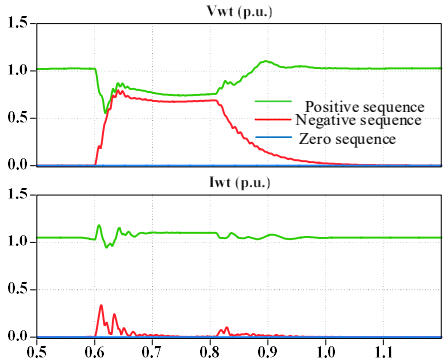

(b)

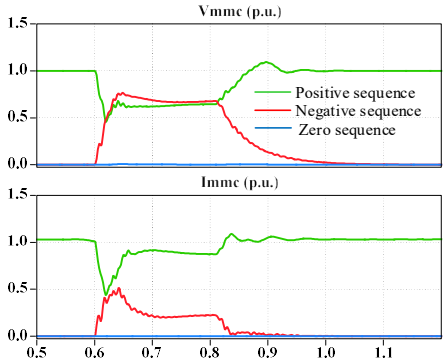

(c)

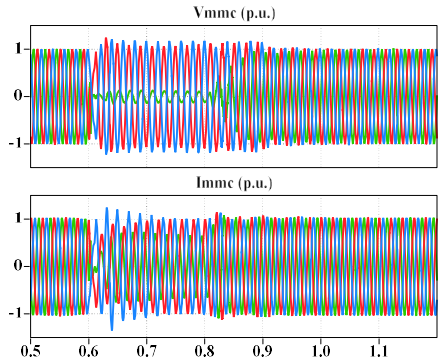

(d)

Fig. 10. Simulation results of the system during a line-to-line fault, the proposed control scheme of the MMC shown in Fig.6 is used. (a) Sequence voltage and current at the fault location. (b) Sequence voltage and current of the WT converter. (c) Sequence voltage and current of the MMC. (d) Time-domain waveform of the MMC.

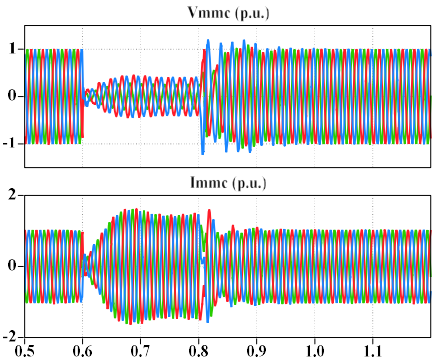

(d)

Fig. 11. Simulation results of the system during a double-line to ground fault, the proposed control scheme of the MMC shown in Fig.6 is used. (a) Sequence voltage and current at the fault location. (b) Sequence voltage and current of the WT converter. (c) Sequence voltage and current of the MMC. (d) Time-domain waveform of the MMC.

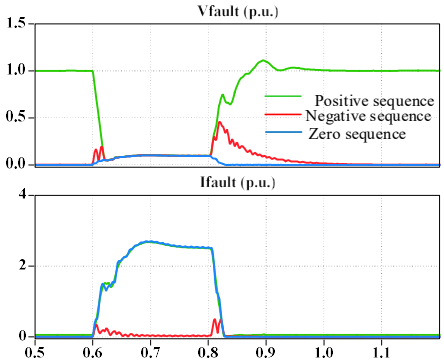

(a)

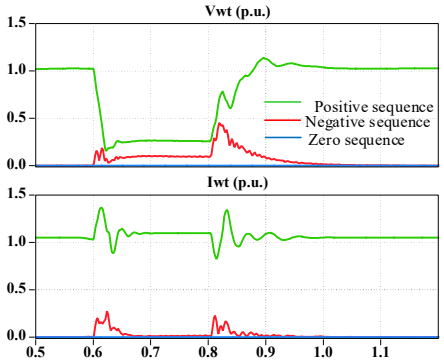

(b)

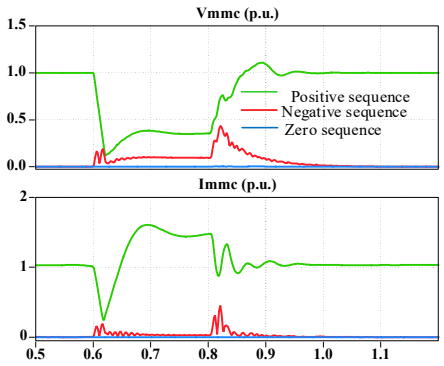

(c)

Fig. 10 and 11 show the simulation results of the system during a line-to-line fault and a double-line to ground fault. The proposed control scheme of the MMC shown in Fig. 6 is adopted. It is clear that the output current of the MMC is limited within 1.5 pu in both cases, which further confirms the effectiveness of the proposed method.

VI. Conclusions

During asymmetrical faults in networks purely based on power electronic converters such as the offshore AC side of an HVDC-connected OWF, the relationship between the positive- and negative-sequence currents at the fault location is constrained by the sequence network. The output sequence currents of the OWF are always controlled based on the grid codes, which, together with the constraints of the faulted sequence network, disables the separate control or limitation of output sequence currents of the MMC-HVDC. This paper proposes FRT control method of the MMC-HVDC by limiting its currents and modulation signals in per-phase basis, while the percentage of the sequence components are not manually specified. The effectiveness of the proposed method is confirmed by time-domain simulations. The findings of this paper have significant implications on, among others, grid code requirements and protection systems functionality, which should be addressed in future work in the field.

References

[1] BDEW Technical Guideline, Generating Plants Connected to the Medium- Voltage Network [EB/OL], June 2008 issue.

[2] European Network for Transmission System Operators for Electricity, "ENTSO-E network code for requirements for grid connection applicable to all generators," Jun. 2012.

[3] Forum Netztechnik/Netzbetrieb im VDE (FNN), "VDE-AR-N 4120:2015-01 Technical requirements for the connection and operation of customer installations to the high-voltage network (TCC HighVoltage)," Jan. 2015.

[4] C.-T. Lee, C.-W. Hsu, and P.-T. Cheng, "A low-voltage ride-through technique for grid-connected converters of distributed energy resources," *IEEE Trans. Ind. Appl.*, vol. 47, no. 4, pp. 1821–1832, Jul./Aug. 2011

[5] O. Goksu, N. A. Cutululis, P. Sorensen, and L. Zeni, "Asymmetrical fault analysis at the offshore network of HVDC connected wind power plants," in *2017 IEEE Manchester PowerTech*, 2017.
[6] Ö. Göksu, N. A. Cutululis, P. Sørensen, "Analysis of HVDC and wind turbine converter response during offshore asymmetrical faults" in 17th *Proc. Wind Integr. Workshop*, 2018.
[7] S. Chaudhary, R. Teodorescu, P. Rodriguez, P. Kjaer, and A. Gole, "Negative sequence current control in wind power plants with VSC-HVDC connection," *IEEE Trans. Sustainable Energy*, vol. 3, no. 3, pp. 535–544, Jul. 2012.
[8] P. M. Anderson and A. A. Fouad, *Analysis of Faulted Power Systems*. Ames, Iowa: Iowa State Univ. Press, 1995